GLS hyperactivity causes glutamate excess, infantile cataract and profound developmental delay

DOI:
10.1093/hmg/ddy330

Document Version
Accepted author manuscript

GLS hyperactivity causes glutamate excess, infantile cataract and profound developmental delay

Lynne Rumping[1,2,3 þ], Federico Tessadori[1,2,4 þ], Petra JW Pouwels[5], Esmee Vringer[1], Jannie P Wijnen[6], Alex A Bhogal[6], Sanne MC Savelberg[1], Karen J Duran[1], Mark JG Bakkers[7], Rúben JJ Ramos[1,2], Peter AW Schellekens[8], Hester Y Kroes[1], Dennis WJ Klomp[6], Graeme CM Black[9,10], Rachel L Taylor[9,10], Jeroen PW Bakkers[4,11], Hubertus CMT Prinsen[1], Marjo S van der Knaap[5], Tobias B Dansen[2,13], Holger Rehmann[2,13], Fried JT Zwartkruis[2,13], Roderick HJ Houwen[3], Gijs van Haaften[1,2], Nanda M Verhoeven-Duif[1,2], Judith JM Jans[1,2*þ], Peter M van Hasselt[3*þ]

[þ] Lynne Rumping and Federico Tessadori contributed equally to this work.

[þ] Judith JM Jans and Peter M van Hasselt contributed equally to this work.

Affiliations:

[1]Department of Genetics, University Medical Center Utrecht, Utrecht University, Utrecht 3584 CX, the Netherlands

[2]Center for Molecular Medicine, University Medical Center Utrecht, Utrecht University, Utrecht 3584 CX, the Netherlands

[3]Department of Pediatrics, University Medical Center Utrecht, Utrecht University, Utrecht 3584 CX, the Netherlands

[4]Hubrecht Institute-KNAW, University Medical Center Utrecht, Utrecht University, Utrecht 3584 CT, the Netherlands

[5]Department of Radiology and Nuclear Medicine, VU University Medical Center, Amsterdam 1081 HV, the Netherlands

[6] Department of Radiology, University Medical Center Utrecht, Utrecht University, Utrecht 3584 CX, the Netherlands

[7]Department of Microbiology and Immunobiology, Harvard Medical School, Boston MA 02115, USA

[8]Department of Ophthalmology, University Medical Center Utrecht, Utrecht University, Utrecht 3584 CX, the Netherlands

[9]Division of Evolution and Genomic Sciences, The University of Manchester, Manchester M139WL, UK

[10]Manchester Centre for Genomic Medicine, St Mary's Hospital, Manchester M139WL, UK

[11]Department of Medical Physiology, University Medical Center Utrecht, Utrecht University, Utrecht 3584 CX, the Netherlands

[12]Department of Child Neurology, VU University Medical Center, Amsterdam 1081 HV, the Netherlands

[13]Molecular Cancer Research, University Medical Center Utrecht, Utrecht University, Utrecht 3584 CX, the Netherlands

Corresponding author*:

Peter M van Hasselt, **Lundlaan 3584 EA Utrecht, the Netherlands,** e-mail address: p.vanhasselt@umcutrecht.nl, tel: +31 88 75 550 56, fax: +31 88 75 553 49

Abstract

Loss-of-function mutations in glutaminase (GLS), the enzyme converting glutamine into glutamate, and the counteracting enzyme glutamine synthetase (GS) cause disturbed glutamate homeostasis and severe neonatal encephalopathy. We report a *de novo* Ser482Cys gain-of-function variant in *GLS* encoding glutaminase associated with profound developmental delay and infantile cataract. Functional analysis demonstrated that this variant causes hyperactivity and compensatory downregulation of GLS expression combined with upregulation of the counteracting enzyme GS, supporting pathogenicity. Ser482Cys-GLS likely improves the electrostatic environment of the GLS catalytic site, thereby intrinsically inducing hyperactivity. Alignment of +/-12.000 GLS protein sequences from >1000 genera, revealed extreme conservation of Ser482, to the same degree as catalytic residues. Together with the hyperactivity, this indicates that Ser482 is evolutionarily preserved to achieve optimal -but submaximal- GLS activity. In line with GLS hyperactivity, increased glutamate and decreased glutamine concentrations were measured in urine and fibroblasts. In the brain (both grey and white matter), glutamate was also extremely high and glutamine almost undetectable, using ultra-high field magnetic resonance spectroscopic imaging. Considering the neurotoxicity of glutamate when present in excess, the strikingly high glutamate concentrations measured in the brain provide an explanation for the developmental delay. Cataract, a known consequence of oxidative stress, was evoked in zebrafish expressing the hypermorphic Ser482Cys-GLS and could be alleviated by inhibition of GLS. The capacity to detoxify reactive oxygen species was reduced upon Ser482Cys-GLS expression, providing an explanation for cataract formation. In conclusion, we describe an inborn error of glutamate metabolism caused by a GLS hyperactivity variant, illustrating the importance of balanced GLS activity.

Introduction

The amino acid glutamate is best known for its role as excitatory neurotransmitter, but also serves as a substrate for other key metabolites, including the anti-oxidant glutathione(1-3). Glutamate homeostasis is mainly warranted by two enzymes: glutamine synthetase (GS; EC 6.3.1.2) and glutaminase (GLS; EC 3.5.1.2). GS converts glutamate into glutamine and is ubiquitously expressed(4). GLS catalyzes the deamination of glutamine into glutamate and ammonia and exists in two isoforms: GLS -present in two splice variants KGA and GAC- mainly expressed in kidney and brain; and GLS2, ubiquitously expressed with the highest expression in the liver(5, 6).

Inborn errors of metabolism are usually due to severe loss of function of the involved enzymes, hence recessive inheritance. In line, a disturbed equilibrium of glutamate and glutamine was described in patients with GS deficiency, clinically resulting in glutamine deficiency, neonatal epilepsy and early death(7). Recently, GLS loss of function has been described to cause lethal epileptic encephalopathy and glutamine excess in two families(8). The description of patients with spastic ataxia and optic atrophy harbouring bi-allelic hypomorphic variants in GLS, suggests a phenotypic spectrum –presumably depending on the degree of residual activity- that is yet to be uncovered(9). Theoretically, glutamate homeostasis can also be disturbed by hyperactivity of either enzyme. This option is commonly disregarded as there are only few examples of genetic variants that induce enzyme hyperactivity, GDH and IDH2 gain of functions(10, 11). These examples indicate that a heterozygous variant is sufficient to induce overall enzyme hyperactivity.

In this study, we characterize a *de novo* hypermorphic heterozygous *GLS* variant found in a patient with infantile onset cataract, skin abnormalities, profound developmental delay and intracerebral glutamate excess. This new inborn error of metabolism illustrates the importance of regulated GLS activity for lens transparency and brain function.

Results

Clinical description

In a female patient, bilateral cataract was diagnosed at the age of 3 months after the parents noticed decreased eye contact and loss of the red light reflex of the pupils on photos (Figure. 1A, S1). The proband is the first child of healthy non-consanguineous parents of Dutch descent (Figure. S1A) as indicated by family history and SNP-array. Gestation and delivery were uneventful. After lens extraction and replacement, eye contact unexpectedly remained absent. By the age of 8 months, delayed development was noted, along with a relative decrease of the head circumference from 0 SD to -2 SD. She developed recurrent dermatological abnormalities on her extremities, cheeks and ears without pruritus, characterized as erythematic subcutaneous nodules of approximately 1 cm (Figure. 1B). Histopathological analysis of these lesions showed deep perivascular and periglandular lymphohistiocytic infiltrates and pronounced leukocytoclasia at the surface of the dermis and focal vacuolar alterations, hyperkeratosis and parakeratosis of the epidermis. A dermatological diagnosis remained inconclusive. Over time, the girl lost the ability to make meaningful sounds and the ability to sit. She developed profound axial hypotonia leading to kyphoscoliosis. Upon arousal she exhibited uncontrolled motoric agitation and self-injurious behavior. Development remained slow paced. At the most recent follow up at the age of 11 years, she was able to use gestures for communication, to understand verbal single component instructions and to steer her own wheelchair.

Identification of the Ser482Cys-GLS de novo variant

Extensive diagnostic workup unexpectedly revealed extremely low glutamine levels and high glutamate levels in both cortex and white matter as detected consistently with quantitative brain proton MRS and MRSI at 1.5Tesla (Figure. 1C, S1B) and recently also shown at 7Tesla (Figure 1D, S1C). Interestingly, CSF and plasma levels were unaffected (Table S1). Brain MRI at age 16 months showed delayed myelination (Figure 1E). Analyses of stored urine samples similarly

showed low concentrations of glutamine and high concentrations of glutamate (Figure. 1F, Table S1). The diagnosis remained enigmatic until trio-based whole exome sequencing (WES) revealed a heterozygous *de novo GLS* missense variant (NC_000002.11:g.191795182C>G). Analysis of WES data using recessive filters yielded no rare homozygous damaging variants. The analysis for compound heterozygosity (including correctness of segregation in parents) yielded two genes hit by rare and possibly damaging variants, but based on gene function, absent links with human disease and the high prevalence within the healthy population, these variants were considered as unlikely to contribute to the phenotypes of the patient (supplementary results). The conservative mutation in *GLS* from serine to cysteine at position 482 NP_055720.3:p.(Ser482Cys) was confirmed by Sanger sequencing (Figure. 1G, supplementary results). Glutaminase mediates the conversion of glutamine into glutamate, therefore this genetic change could only be explained if the encoded protein would be hyperactive.

Ser482Cys-GLS leads to GLS hyperactivity

The effect of the Ser482Cys-*GLS* variant on the activity of the GLS enzyme was assessed in fibroblasts from the patient by quantification of intracellular glutamine and glutamate. The *GLS* variant indeed resulted in an increased intracellular glutamate:glutamine ratio (Figure. 2A, 2B, S2A). To validate enhanced catalytic activity of the GLS variant, a HEK293 cell model with inducible expression of Ser482Cys-*GLS* (KGA, the long splice variant) was generated. Induction of Ser482Cys-*GLS* again strongly increased the glutamate:glutamine ratio while induction of wildtype *GLS* had no effect (Figure. 2C, 2D, S2B). Inhibition of GLS with CB-839 resulted in normalization of glutamate and glutamine concentrations in both fibroblasts and HEK293 cells, providing additional evidence that the Ser482Cys-*GLS* variant leads to GLS hyperactivity.

GLS hyperactivity leads to metabolic compensatory mechanisms

Protein expression of both GLS splice variants KGA and GAC in patient fibroblasts was decreased -rather than increased- compared to controls, ruling out that increased GLS activity was due to increased protein availability. Conversely, the observed down-regulation of GLS protein expression suggests it served as a compensatory mechanism aiming at normalizing glutamine and glutamate concentrations (Figure. 2B). In support, introduction of Ser482Cys-*GLS* in HEK293 cells also evoked decreased GAC expression levels (Figure. 2D, S2C). Furthermore, CB-839-induced GLS inhibition restored GLS expression. GLS expression could also be restored by normalization of glutamate levels through depletion of extracellular glutamine, pointing to glutamate as a regulator of GLS expression (Figure. 2D). Finally, the observation that protein levels of the reciprocal enzyme GS increased upon expression of Ser482Cys-GLS -an effect that could also be reversed through CB-839-mediated GLS inhibition (Figure. 2B, 2D)- underlines that cellular efforts were aimed at normalizing glutamine and glutamate concentrations.

Ser482 functions as a highly conserved intrinsic restrictor of glutaminase activity

Ser482 is located near the catalytic site of GLS, but does not have an identified role in the catalytic process itself (12). Alignment of +/- 12.000 GLS protein sequences from > 1000 genera, revealed that Ser482 is a residue with an extremely high degree of evolutionary conservation (conservation score >0.98) along with residues directly involved in the catalytic process (Figure. 2E). The Ser482Cys substitution is absent in healthy populations in the databases GoNL(13), gnomAD(14), ClinVar(15) and ExAC(16) and is expected to be tolerated without overall disturbances of the protein fold. Interestingly, substitution by cysteine -containing a sterically more demanding and less polar thiol group than serine- changes the electrostatic environment of Tyr466, one of the catalytic residues that protonates glutamine and thereby accelerates deamination into glutamate. This change is likely to enhance the propensity

for proton donation and thereby to increase the speed of the reaction (Figure. 2F, S3, Supplemental discussion).

GLS hyperactivity decreases redox buffer capacity

Oxidative stress is a known consequence of glutamate excess and a common cause of cataract and neuronal injury(17, 18). In HEK293 cells expressing Ser482Cys-*GLS,* clearance of a sub-lethal pulse of hydrogen peroxide was impaired with normal basal reactive oxygen species (ROS) levels. (Figure 3). This indicates that Ser482Cys-*GLS* results in a lower capacity for ROS scavenging.

Ser482Cys-GLS induces lens opacification

To explore the causal relationship between Ser482Cys-*GLS* expression and cataract, we examined the effect of this variant in developing zebrafish embryos. Lens transparency at 5 days post fertilization (dpf) in zebrafish embryos injected with Ser482Cys-*GLS* cDNA was compared to that in control embryos injected with wildtype *GLS* or uninjected embryos (Figure. S4A). Of the embryos expressing the Ser482Cys-GLS variant, 34/47 (72%) developed structural opacities in the lens, which were not observed in any of the control embryos (Figure. 4A-C, S4B-D). GLS inhibition with CB-839 from 6 hours post fertilization (hpf) resulted in profoundly decreased formation of structural opacities in the lens of the Ser482Cys-*GLS* zebrafish embryos (Figure. 4D, Figure. S4E).

Discussion

We characterize a *de novo* heterozygous, hyperactive *GLS* variant found in a patient with infantile onset cataract, skin abnormalities, profound developmental delay and intracerebral glutamate excess. The increased conversion of glutamine into glutamate observed upon introduction of this variant provides a compelling explanation for the strikingly elevated glutamate levels in cerebro and -in view of the central role of glutamate in brain functioning-

likely explains the developmental delay. Furthermore, zebrafish studies unexpectedly reveal that introducing the hypermorphic GLS variant induces lens opacities. Together with the observations that the lens opacities are amenable to GLS inhibition, this supports a role for glutaminase activity in cataract formation.

Inborn errors of metabolism are usually due to bi-allelic or mono-allelic loss-of-function variants with few exceptions. Of these, hyperinsulinism-hyperammonemia syndrome is caused by increased sensitivity of the enzyme GDH to allosteric activation and D-2-hydroxyglutaric aciduria is caused by a neomorphic function of the enzyme IDH2(19, 20). The variant described here truly increases enzymatic activity (Supplemental discussion) likely due to an improved electrostatic environment of the GLS catalytic site. To the best of our knowledge, this nature of hypermorphic gain-of-function in which activity is intrinsically increased by improvement of the catalytic machinery has not been described before. Although rare by nature, it is possible that the current paradigm –heterozygous variants in enzyme encoding genes are usually harmless- hampers identification of comparable disease causing hypermorphic variants in enzyme encoding genes.

The cellular efforts, aimed at counteracting the effects of the hyperactive enzyme by decreasing GLS protein availability while increasing the reciprocal enzyme GS, underline that increased GLS activity is detrimental. Our data underline the observation by Krebs in 1935 that glutamate acts as a sensor for GLS regulation and reveal that glutamate not only affects GLS enzyme kinetics but also its expression. The extremely high degree of conservation of the hypermorphic residue across > 1000 genera -comparable only to residues directly involved in the enzymatic conversion of glutamine into glutamate- suggests that the serine residue serves as a built-in restrictor, ensuring submaximal activity rather than maximal enzyme activity of GLS.

A point of interest is the observation that the ratio between glutamate and glutamine was increased in brain and urine, while it remained unaltered in CSF and plasma. We postulate that this discrepancy is explained by the degree to which glutamine and glutamate levels are controlled by GLS. Tissues with abundant expression of GLS -neurons and kidney- are mainly under GLS control (6). The relative importance of GLS within the brain is illustrated by a high glutamate/glutamine ratio (2:1) in normal population (21). GLS overactivity may be masked in other tissues in which GLS is only one of several players -including GS- that together regulate glutamine and glutamate levels. The reduced importance of GLS in plasma is reflected by the significantly lower ratio of glutamate/glutamine (1:15) (22). Further supporting this hypothesis, the ratio is even lower (~1:100) in CSF, which is produced by choroid plexus from plasma by glial cells that are known to have high GS expression (4) (22). The striking contrast between CSF and brain could be regarded as a cautionary note: CSF should not be readily regarded as a proxy for the brain.

Under physiological conditions, glutamate is important for redox homeostasis as it is the precursor of the anti-oxidant glutathione(2). Glutamate excess, however, is associated with oxidative stress, a common cause of cataract and neuronal damage(17, 18). We show that GLS hyperactivity indeed leads to decreased capacity for redox buffering, which can result in oxidative stress. We therefore postulate that glutamate excess contributes to the ophthalmologic phenotype of our patient. In the aqueous humor -nourishing the lens- glutamate concentrations are strictly regulated and even kept low by metabolism and transport(23). Exposure to glutamate causes cataract in chick and rat embryos(17, 24, 25). In line with the phenotype of the affected patient, zebrafish expressing Ser482Cys-GLS develop lens opacities which could be largely prevented by GLS inhibition. Interestingly, neurons and lens cells are both of ectodermal origin, as is the skin, and share similarities in expression and regulation of glutamate receptors, supporting the notion that disturbed glutamate homeostasis not only affects the brain, but also

skin and lens(26). Glutamate excitotoxicity has been associated with epilepsy, numerous neurodegenerative diseases, self-injury and agitated behavior(18, 27). The measured glutamate excess in the brain of our patient might therefore provide a plausible explanation for the self-injury behavior and developmental delay of our patient.

Interestingly, other defects affecting glutamate homeostasis lead to neurological phenotypes as well. Under physiological circumstances, homeostasis of glutamine and glutamate in the brain is strictly regulated by neuronal GLS and astrocytic GS via the glutamine-glutamate shuttle(4). GLS loss of function variants lead to a phenotypic spectrum. The first description was of a late childhood onset disease, including optic atrophy and spastic ataxia(9). Recently, bi-allelic loss of function variants in *GLS* were described to cause lethal, neonatal onset encephalopathy characterized by respiratory failure, status epilepticus and early death within weeks after birth(8). These patients had simplified gyral patterns and showed destructions of initially normal appearing brain structures. Both the reported hiccups during pregnancy and the simplified gyral patterns on imaging suggest the damage has its onset prenatally. Given the truncating mutations present in the latter phenotype it is tempting to speculate a dose effect relationship explaining the phenotypic spectrum. This inborn error –together with GLS hyperactivity- illustrates the importance of proper GLS activity for both brain physiology and morphology.

Deficiency of GS –performing the reversed reaction of GLS- results in decreased glutamine levels but normal glutamate levels and hyperammonemia. This has been reported in three individuals which exhibited neonatal encephalopathy, seizures and respiratory failure and early death(28). The absence of epilepsy in our patient with GLS hyperactivity despite increased glutamate levels on brain MRSI is unexpected as glutamate excitotoxicity is considered a critical factor in the initiation of epileptic seizures(29). Seizures can be provoked by either increased glutamate release into the synaptic cleft or decreased re-uptake or recycling from the

synaptic cleft, which implies that glutamate levels in the synaptic cleft of our patient are unaffected despite overall brain glutamate abundance. The phenotypic neurological spectrum of these patients show the importance of strictly regulated glutamate homeostasis for neurological functioning.

A limitation of our study is that only a single patient with a hyperactive variant in GLS could be identified. Hyperactive variants are extremely uncommon, especially in a well conserved catalytic area like in GLS. Intolerance to loss-of-function in GLS is likely high, meaning that mutations will likely be lethal. These factors contribute to a limited patient pool. While definite pathogenic conclusions are considered difficult based on evidence from unique subjects, when adequately studied, these cases can be regarded as experiments of nature and provide invaluable insights. Such is the case here, were we provide strong evidence that GLS hyperactivity causes a new metabolic disorder of glutamate metabolism. Our study furthermore provides insight into the regulation of GLS activity and illustrates the importance of appropriate GLS activity for human brain function, skin and lens transparency.

Materials and Methods

Clinical phenotyping, diagnostics and exome sequencing

Clinical phenotyping was performed and diagnostic tests were requested by metabolic pediatricians, clinical geneticists, an ophthalmologist, neurologists and dermatologist. Amino acids analyses in urine were performed on a Biochrom30 analyzer. In the brain, these were determined with quantitative Magnetic Resonance Spectroscopic (MRS) and Spectroscopic Imaging (MRSI) at 1.5Tesla at age 2 and 3 years and with MRSI at 7Tesla at age 14 years. Genetic analysis was performed by trio-based whole-exome sequencing and Sanger sequencing. See supplementary methods for details.

GLS activity

GLS activity was determined in patient fibroblasts and in human embryonic kidney 293 (HEK293) cells stably transfected with either wildtype or Ser482Cys-*GLS* (KGA isoform) or an empty vector, in absence or presence of different concentrations of the allosteric GLS inhibitor CB-839(30). GLS activity was defined as the formation of glutamate from glutamine, quantified by ultra-performance liquid chromatography tandem mass spectrometry(31). Protein expression was assessed by Western Blot.

Conservation analysis

Sequences homologous to human GLS from the non-redundant protein collection at NCBI were aligned in SeaView(32). Obvious partial sequences as well as all pdb sequences were removed which resulted in about 12.000 sequences. The consensus were determined in JalView(33) and fraction of the modal residue in a column were used for generating a color gradients which was mapped onto the GLS structure as a measure of conservation (consensus score).

Reactive oxygen species

ROS-levels were quantified by flow cytometry (BD FACSCalibur^{TM}) as previously described in wildtype *GLS* or Ser482Cys-*GLS* transfected HEK293 cells(34).

Animal model

Zebrafish *(Danio rerio)* embryos were microinjected at the 1-cell stage with DNA constructs coding for wildtype or Ser482Cys-GLS (KGA isoform). Uninjected zebrafish embryos were used as controls. The embryos were kept under standard laboratory conditions, either in the absence or in the presence of the GLS inhibitor CB-839, prior to assessment of glutamine and glutamate concentrations and lens opacity at 5 days post fertilization (dpf).

Statistics

311 Statistical analyses were performed by ANOVA, post-hoc Tukey's test using IBM SPSS
312 statistics 21.

313

314 *Study approval*

315 The proband's parents provided written informed consent for all aspects of the study.
316 Zebrafish experiments were carried out in accordance with the guidelines of the Animal
317 Experimentation Committee of the Royal Netherlands Academy of Arts and Sciences
318 (KNAW).

319 For more detailed information, see supplementary materials and methods.

320

321 **Acknowledgements**

322 We are grateful for the contribution of the patient's family to this study. We would like to thank
323 Willem Hoefakker, Birgit Schiebergen-Bronkhorst, Ans Geboers, Mirjam van Aalderen,
324 Annique Claringbould, Elise Meijer and Lida Lughthart for their great technical assistance. We
325 also thank Sahar Nassirpour and Paul Chang for providing assistance in reconstructing the
326 7Teska MRSI data. This work was funded by ODAS and Erfelijke Stofwisselingsziekten
327 Nederlands taalgebied (ESN).

328 The authors declare no competing financial interests.

329

330 **Author contributions**

331 LR, FT, HCMTP, FJTZ, GH, NMVD, JJMJ and PMH contributed to the concept and design of
332 the study. PMH and JJMJ coordinated the study. PJWP, HYK, HCMTP, MSK, GH, NMVD,
333 JJMJ and PMH provided clinical phenotyping, diagnostics, patient care and (genetic)
334 counseling. LR, FT, PJWP, EV, JPW, AAB, SMCS, KJD, MJGB, RJJR, PAWS, DWJK,

GCMB, RLT, JPWB, TBD, HR and FJTZ contributed to the acquisition and interpretation of the data. LR and FT wrote the manuscript and all co-authors critically revised the manuscript and provided final approval of the manuscript to be published.

References

1 Curtis, D.R., Phillis, J.W. and Watkins, J.C. (1960) The chemical excitation of spinal neurones by certain acidic amino acids. *J Physiol*, **150**, 656-682.

2 Lu, S.C. (2009) Regulation of glutathione synthesis. *Mol Aspects Med*, **30**, 42-59.

3 Nedergaard, M., Takano, T. and Hansen, A.J. (2002) Beyond the role of glutamate as a neurotransmitter. *Nat Rev Neurosci*, **3**, 748-755.

4 Bak, L.K., Schousboe, A. and Waagepetersen, H.S. (2006) The glutamate/GABA-glutamine cycle: aspects of transport, neurotransmitter homeostasis and ammonia transfer. *J Neurochem*, **98**, 641-653.

5 Curthoys, N.P. and Watford, M. (1995) Regulation of glutaminase activity and glutamine metabolism. *Annu Rev Nutr*, **15**, 133-159.

6 Aledo, J.C., Gomez-Fabre, P.M., Olalla, L. and Marquez, J. (2000) Identification of two human glutaminase loci and tissue-specific expression of the two related genes. *Mamm Genome*, **11**, 1107-1110.

7 Spodenkiewicz, M., Diez-Fernandez, C., Rufenacht, V., Gemperle-Britschgi, C. and Haberle, J. (2016) Minireview on Glutamine Synthetase Deficiency, an Ultra-Rare Inborn Error of Amino Acid Biosynthesis. *Biology (Basel)*, **5**.

8 Rumping, L., Büttner, B., Maier, O., Rehmann, H., Lequin, M., Schlump, J., Schmitt, B., Schiebergen-Bronkhorst, B.G.M., Prinsen, B.H. and Losa, M. (UNPUBLISHED (accepted 2018)) Loss of function of GLS disturbs glutamate-glutamine homeostasis and leads to early lethal epileptic encephalopathy. *JAMA-NEU*, in press.

9 Lynch, D.S., Chelban, V., Vandrovcova, J., Pittman, A., Wood, N.W. and Houlden, H. (2018) GLS loss of function causes autosomal recessive spastic ataxia and optic atrophy. *Ann Clin Transl Neurol*, **5**, 216-221.

10 Kapoor, R.R., Flanagan, S.E., Fulton, P., Chakrapani, A., Chadefaux, B., Ben-Omran, T., Banerjee, I., Shield, J.P., Ellard, S. and Hussain, K. (2009) Hyperinsulinism-hyperammonaemia syndrome: novel mutations in the GLUD1 gene and genotype-phenotype correlations. *Eur J Endocrinol*, **161**, 731-735.

11 Yang, H., Ye, D., Guan, K.L. and Xiong, Y. (2012) IDH1 and IDH2 mutations in tumorigenesis: mechanistic insights and clinical perspectives. *Clin Cancer Res*, **18**, 5562-5571.

12 Brown, G., Singer, A., Proudfoot, M., Skarina, T., Kim, Y., Chang, C., Dementieva, I., Kuznetsova, E., Gonzalez, C.F., Joachimiak, A. *et al.* (2008) Functional and structural characterization of four glutaminases from Escherichia coli and Bacillus subtilis. *Biochemistry*, **47**, 5724-5735.

13 Genome of the Netherlands, C. (2014) Whole-genome sequence variation, population structure and demographic history of the Dutch population. *Nat Genet*, **46**, 818-825.

14 Lek M, K.K., Minikel EV. (Accessed March 20, 2018) 2016:285-291, N. (ed.), in press.

15 Landrum, M.J., Lee, J.M., Benson, M., Brown, G.R., Chao, C., Chitipiralla, S., Gu, B., Hart, J., Hoffman, D., Jang, W. *et al.* (2018) ClinVar: improving access to variant interpretations and supporting evidence. *Nucleic Acids Res*, **46**, D1062-D1067.

16 Lek, M., Karczewski, K.J., Minikel, E.V., Samocha, K.E., Banks, E., Fennell, T., O'Donnell-Luria, A.H., Ware, J.S., Hill, A.J., Cummings, B.B. *et al.* (2016) Analysis of protein-coding genetic variation in 60,706 humans. *Nature*, **536**, 285-291.

17 Spector, A. (1995) Oxidative stress-induced cataract: mechanism of action. *FASEB J*, **9**, 1173-1182.

18 Dong, X.X., Wang, Y. and Qin, Z.H. (2009) Molecular mechanisms of excitotoxicity and their relevance to pathogenesis of neurodegenerative diseases. *Acta Pharmacol Sin*, **30**, 379-387.

19 Grimaldi, M., Karaca, M., Latini, L., Brioudes, E., Schalch, T. and Maechler, P. (2017) Identification of the molecular dysfunction caused by glutamate dehydrogenase S445L mutation responsible for hyperinsulinism/hyperammonemia. *Hum Mol Genet*, **26**, 3453-3465.

20 Kranendijk, M., Salomons, G.S., Gibson, K.M., Van Schaftingen, E., Jakobs, C. and Struys, E.A. (2011) A lymphoblast model for IDH2 gain-of-function activity in d-2-hydroxyglutaric aciduria type II: novel avenues for biochemical and therapeutic studies. *Biochim Biophys Acta*, **1812**, 1380-1384.

21 Bank van de, B.L., Emir, U.E., Boer, V.O., Asten van, J.J.A., Maas, M.C., Wijnen, J.P. and Kan, H.E. (2015) Multi-center reproducibility of neurochemical profiles in the human brain at 7 Tesla. *NMR Biomed*, **28**, 306-316.

22 Blau, N., Duran, M. and Gibson, K.M. (2008) *Laboratory Guide to the Methods in Biochemical Genetics*. Springer, Heidelberg Berlin.

23 Hu, R.G., Lim, J.C., Kalloniatis, M. and Donaldson, P.J. (2011) Cellular localization of glutamate and glutamine metabolism and transport pathways in the rat ciliary epithelium. *Invest Ophthalmol Vis Sci*, **52**, 3345-3353.

24 Kawamura, M. and Azuma, N. (1992) Morphological studies on cataract and small lens formation in neonatal rats treated with monosodium-L-glutamate. *Ophthalmic Res*, **24**, 289-297.

25 Laszczyk, W.A. (1975) Development of Cataract as the Effect of Glutamic Acid Administration to Chick Embryo. *Ophthalmic Res*, **7**, 432-439.

26 Farooq, M., Kaswala, R.H., Kleiman, N.J., Kasinathan, C. and Frederikse, P.H. (2012) GluA2 AMPA glutamate receptor subunit exhibits codon 607 Q/R RNA editing in the lens. *Biochem Biophys Res Commun*, **418**, 273-277.

27 Brodie, M.J., Besag, F., Ettinger, A.B., Mula, M., Gobbi, G., Comai, S., Aldenkamp, A.P. and Steinhoff, B.J. (2016) Epilepsy, Antiepileptic Drugs, and Aggression: An Evidence-Based Review. *Pharmacol Rev*, **68**, 563-602.

28 Haberle, J., Gorg, B., Rutsch, F., Schmidt, E., Toutain, A., Benoist, J.F., Gelot, A., Suc, A.L., Hohne, W., Schliess, F. *et al.* (2005) Congenital glutamine deficiency with glutamine synthetase mutations. *N Engl J Med*, **353**, 1926-1933.

29 Barker-Haliski, M. and White, H.S. (2015) Glutamatergic Mechanisms Associated with Seizures and Epilepsy. *Cold Spring Harb Perspect Med*, **5**, a022863.

30 Gross, M.I., Demo, S.D., Dennison, J.B., Chen, L., Chernov-Rogan, T., Goyal, B., Janes, J.R., Laidig, G.J., Lewis, E.R., Li, J. *et al.* (2014) Antitumor activity of the glutaminase inhibitor CB-839 in triple-negative breast cancer. *Mol Cancer Ther*, **13**, 890-901.

31 Prinsen, H.C., Schiebergen-Bronkhorst, B.G., Roeleveld, M.W., Jans, J.J., de Sain-van der Velden, M.G., Visser, G., van Hasselt, P.M. and Verhoeven-Duif, N.M. (2016) Rapid quantification of

underivatized amino acids in plasma by hydrophilic interaction liquid chromatography (HILIC) coupled with tandem mass-spectrometry. *J Inherit Metab Dis*, **39**, 651-660.

32 Gouy, M., Guindon, S. and Gascuel, O. (2010) SeaView version 4: A multiplatform graphical user interface for sequence alignment and phylogenetic tree building. *Mol Biol Evol*, **27**, 221-224.

33 Waterhouse, A.M., Procter, J.B., Martin, D.M., Clamp, M. and Barton, G.J. (2009) Jalview Version 2--a multiple sequence alignment editor and analysis workbench. *Bioinformatics*, **25**, 1189-1191.

34 Jelluma, N., Yang, X., Stokoe, D., Evan, G.I., Dansen, T.B. and Haas-Kogan, D.A. (2006) Glucose withdrawal induces oxidative stress followed by apoptosis in glioblastoma cells but not in normal human astrocytes. *Mol Cancer Res*, **4**, 319-330.

35 Pouwels, P.J., Brockmann, K., Kruse, B., Wilken, B., Wick, M., Hanefeld, F. and Frahm, J. (1999) Regional age dependence of human brain metabolites from infancy to adulthood as detected by quantitative localized proton MRS. *Pediatr Res*, **46**, 474-485.

36 Kraulis, P.J. (1991) Molscript - a program to produce both detailed and schematic plots of protein structures. *Journal of Applied Crystallography*, **24**, 946-950.

37 Merritt, E.A. and Murphy, M.E. (1994) Raster3D Version 2.0. A program for photorealistic molecular graphics. *Acta Crystallogr D Biol Crystallogr*, **50**, 869-873.

Figure legends

Figure 1. Identification of a *GLS de novo* variant in a patient with bilateral infantile cataract. (**A**) Photographs of the eyes of the patient at different ages depict a decrease in light reflex, indicating the formation of cataract before the age of three months. (**B**) Dermatological manifestation of erythematic nodules of approximately 1 cm, here on the dorsum of the foot. (**C**) Glutamine and glutamate concentrations assessed by Magnetic Resonance Spectroscopy (1.5 Tesla, both STEAM, TR/TM/TE 6000/30/20 ms, and PRESS, TR/TE 3000/30 ms) in the parietal cortex and white matter of the patient at ages 2 and 3 years. The normal range, +/- 2 SD from mean based on control values of children between 2 and 5 years of age(35) is depicted

444 in grey. Data represent concentrations in single voxel MRS (o) and in multiple voxels from
445 MRSI (x). (**D**) Maps of glutamine (middle panel) and glutamate (right panel) levels in the brain
446 of the patient at age 14 years (lower row) and a control (top row), generated from 2D MRSI
447 acquisitions (7T, pulse-acquire, matrix 44x44, 0.5x0.5x1.0 cm^3, TR/TE 300/2.5 ms) overlaid
448 on anatomical magnetic resonance images (left panel). (**E**) Magnetic resonance imaging of the
449 patient at age 16 months, revealing delayed myelination. The transverse T1-weighted image
450 (left) shows the myelinated cerebral white matter as white. The FLAIR (middle) and T2-
451 weighted (right) images have a lack of contrast between cerebral hemispheric white matter and
452 cortex, indicating that myelination is incomplete. Better myelinated structures, including corpus
453 callosum and internal capsule, have a lower signal. (**F**) Urinary excretion of glutamate and
454 glutamine, presented as ratios on a logarithmic scale in the urine of the patient (black dots)
455 compared to controls (white dots). (**G**) DNA Sanger sequencing trio analysis shows the
456 Ser482Cys-*GLS de novo* variant in the patient, which is absent in the unaffected parents. The
457 underlined sequence indicates the nucleic acid change causing the substitution of the amino
458 acid serine for cysteine.

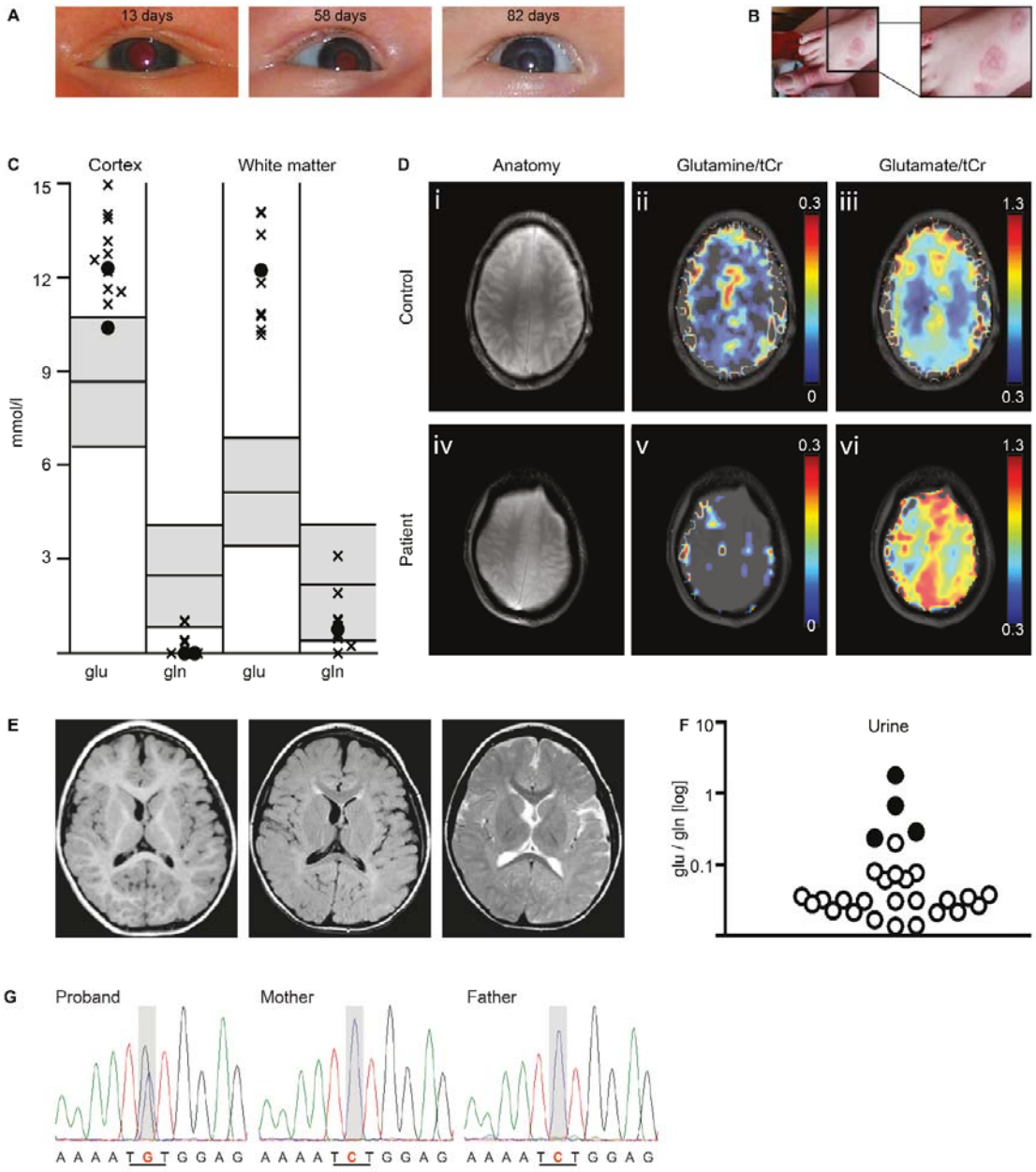

Figure 2. Impact of Ser482Cys-GLS on enzyme activity, expression and structure. (**A-C**) Glutamate and glutamine values measured with UPLC-MS/MS, expressed as the ratio of glutamate:glutamine in (**A**) fibroblasts of 3 controls (white) and the proband expressing Ser482Cys-GLS (black) and (**C**) HEK293 cells stably transfected with an empty vector (checked), wildtype *GLS* (white) or Ser482Cys-*GLS* (black). Cells containing the variant were untreated (highlighted) or treated with 0.1 μM, 0.5 μM, 1 μM or 10 μM CB-839. Data represent the mean of biological triplicates with standard deviations. *p<0.05 (ANOVA, Tukey's test) **p<0.01 (ANOVA, Tukey's test) ns: not significant. (**B-D**) Western blots of both GLS splice variants -kidney type glutaminase (KGA) and glutaminase C (GAC)- and GS. (**B**) In fibroblasts of 3 controls and the patient expressing Ser482Cys-GLS, the latter treated with CB-839 corresponding to panel a. The mean of the expression levels in control fibroblasts is arbitrarily set at 1. (**D**) In HEK293 cells stably transfected with an empty vector (EV), wildtype *GLS* (Wt) or Ser482Cys-*GLS* (KGA), the latter treated with CB-839 (corresponding to panel c) or deprived from glutamine to normalize glutamate concentrations (glu=). Expression levels in cells expressing wildtype GLS are arbitrarily set at 1. Results are normalized to actin or GADPH. Analyses performed on the same blot are delineated. (**E**) Conservation analysis of GLS, in which residues with conservation scores from 0 to 0.98 are represented by a color gradient from yellow to red and the most conserved residues (> 0.98) are represented in black. These residues are clustered around the catalytic site and most of them are directly involved in the catalytic reaction: Ala339 (0.994), Lys481 (0.992), Asn335 (0.991), Lys289 (0.990), Ser286 (0.990), Tyr414 (984), Tyr466 (0.986) and Asn388 (0.983). Among these is Ser482 (0.983), indicated by the asterisk symbol. Glutamine is shown in green ball-an-stick representation. Glycine and proline residues -often conserved for pure structural reasons- were omitted and are shown in light grey. (**F**) Zoom-in on the catalytic site of GLS in complex with glutamine (green) shows that Ser482 (magenta) is located near the catalytic site. The deamination reaction of

490 glutamine is initiated by a nucleophilic attack of Ser286 on C^{δ} of glutamine (red arrow) and is
491 accelerated by Tyr466 via protonation (black arrows indicate proton transfer). The electrostatic
492 environment of Tyr466 is determined by the hydroxyl-group of Ser482 (yellow dotted line).
493 Hydrogen bonds are shown by dotted black lines. Supplemental Figure. 3 provides additional
494 insight into the enzymatic reaction and the possible consequences of the Ser482Cys
495 substitution. Figures are based on pdb entry 3vp0 and were generated with molscript(36) and
496 raster3D(37)

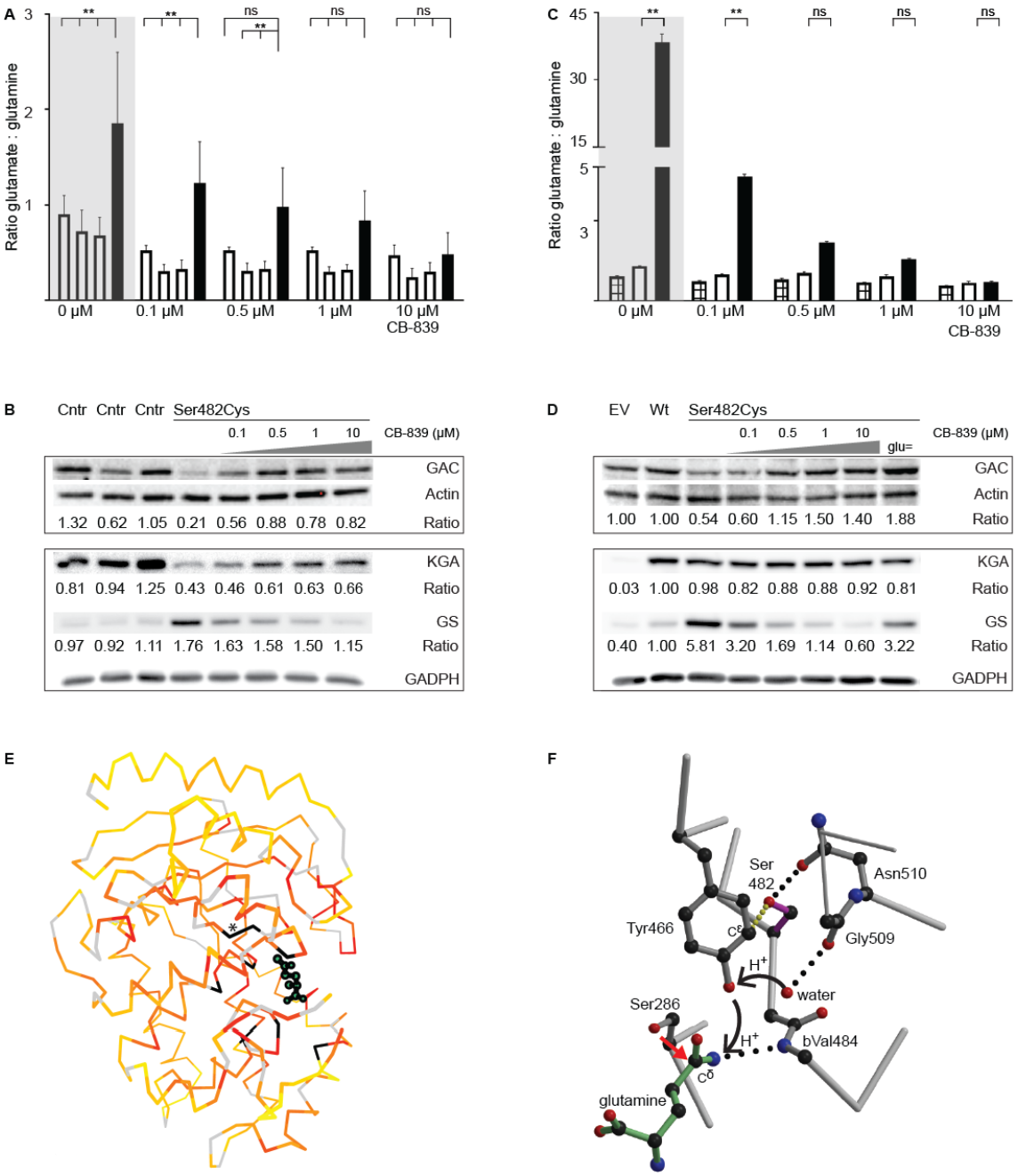

Figure 3. ROS levels and redox buffering capacity. HEK293 cells were transfected with wildtype *GLS* or Ser482Cys-*GLS*, with and without exposure to H_2O_2, measured with flow cytometry, using CM-H_2DCF-DA. (**A**) Histograms of non-induced (-dox, black) and induced (+dox, grey) cells, showing the shift in CM-H_2DCF fluorescence intensity after induction with doxycycline and exposure to 50 µM H_2O_2, Data are normalized to total cell counts and are representative for biological triplicates. (**B**) Ratio of the median CM-H_2DCF fluorescence intensities of cells induced with doxycycline over uninduced cells. Data present the mean of biological triplicates with standard errors of the mean. ns: not significant *p<0.05 (ANOVA, Tukey's test).

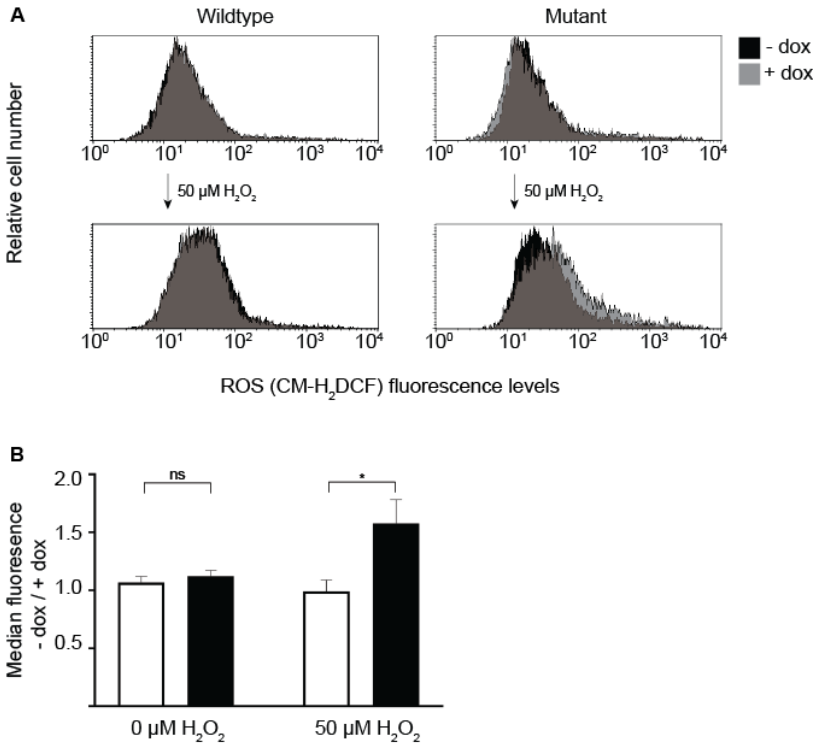

Figure 4. Lens opacity of zebrafish expressing Ser482Cys-*GLS*. Representative images of the lenses of 5 dpf zebrafish embryos of (**A**) uninjected n=30 or injected with vectors containing (**B**) wildtype *GLS* cDNA n=28 or (**C**) Ser482Cys-*GLS* cDNA KGA isoform n=63. (**D**) Zebrafish embryos expressing Ser482Cys-GLS were treated with 10 μM CB-839 from 6 hpf n=10. Opacities in the lens are indicated with arrows. See Supplemental Figure. 4 for all images. Images were obtained with a fluorescence microscope. Linear image editing was performed.